DOI 10.1007/s11595-016-1491-8

Numerical Simulation on Interfacial Creep Failure of Dissimilar Metal Welded Joint between HR3C and T91 Heat-Resistant Steel

ZHANG Jianqiang[1], TANG Yi[2], ZHANG Guodong[1], ZHAO Xuan[1], GUO Jialin[1], LUO Chuanhong[1]

(1. Key Laboratory of Hubei Province of Water Jet Theory and New Technology, Wuhan University, Wuhan 430072, China; 2. Research Institute of Nuclear Power Operation, Wuhan 430074, China)

Abstract: The maximum principal stress, von Mises equivalent stress, equivalent creep strain, stress triaxiality in dissimilar metal welded joints between austenitic (HR3C) and martensitic heat-resistant steel (T91) are simulated by FEM at 873 K and under inner pressure of 42.26 MPa. The results show that the maximum principal stress and von Mises equivalent stress are quite high in the vicinity of weld/T91 interface, creep cavities are easy to form and expand in the weld/T91 interface. There are two peaks of equivalent creep strains in welded joint, and the maximum equivalent creep strain is in the place 27-32 mm away from the weld/T91 interface, and there exists creep constrain region in the vicinity of weld/T91 interface. The high stress triaxiality peak is located exactly at the weld/T91 interface. Accordingly, the weld/T91 interface is the weakest site of welded joint. Therefore, using stress triaxiality to describe creep cavity nucleation and expansion and crack development is reasonable for the dissimilar metal welded joint between austenitic and martensitic steel.

Key words: dissimilar metal welded joint; maximum principal stress; equivalent stress; creep strain; stress triaxiality

1 Introduction

New type austenitic heat-resistant steel HR3C has been widely used in the final stages of super heaters and reheaters of ultra-super critical(USC) fossil-fired power plants because it is excellent in resistance to smoke corrosion and oxidation, high temperature strength and weldability[1-2]. For economic considerations, martensitic heat-resistant steel T91 is used in the earlier stages where the temperatures are lower, thus there is a need for dissimilar metal welded joint (DMWJ). In addition, DMWJ has been extensively utilized in boiler, pressure vessels, petrochemical plant, and nuclear reactors. It has long been recognized that DMWJ has a potential problem because large thermal stress can generate at the joint due to the difference in thermal expansion coefficient of the jointed metals, and localized metallurgical changes can occur as a result of long term elevated temperature service which can render the interface region between weld and base metal more susceptible to creep damage and premature failure. Such failures are costly and contribute to the overall failure rate[3-5].

There are differences in the compositional gradient, the coefficient of thermal expansion (CTE) and thermal stress of welded joint between austenitic and martensitic steel. Accordingly, the premature failures of austenitic/martensitic joint have occurred frequently. Nucleation and propagation of creep cracks along the interface between weld and martensitic steel during service have been considered responsible for the failures, and the filler metals of welds is an important factor in premature service failure in these joints[6-9].

In this paper, the maximum principal stress, von Mises equivalent stress, equivalent strain and stress triaxiality in dissimilar welded joints between austenitic heat-resistant steel (HR3C) and martensitic heat-resistant steel (T91) are simulated by FEM at 873 K and under inner pressure of 42.6 MPa. Nucleation and propagation characteristics of creep cavities of dissimilar welded joints have been analyzed.

(Received: Nov. 17, 2015; Accepted: May 21, 2016)

ZHANG Jianqiang(张建强): Assoc. Prof.; E-mail: zhangjq123456@163.com

Funded by the National Natural Science Foundation of China (No.51374154)

2 FEM model

2.1 Experimental materials and welding process

The experimental materials were austenitic heat resistance steel HR3C and martensitic heat-resistant steel T91 tubes. The outer diameter, wall thickness and length of tubes were 57, 7 and 120 mm, respectively. The filler metal was ERNiCr-3, and the chemical compositions of base metals and filler metals are shown in Table 1.

TIG welding was used in welding experiments, single V butt joint was used, groove angle was 65° and the root face and gap were zero. Welding layers and passes were 5 and 9, respectively. Weld reinforcements of outer and inner surface were 2 and 1.5 mm, weld widths of outer and inner surfaces were 12 and 6 mm respectively. The preheat temperature was 448 K, and post welding heat treatment (PWHT) was not used. The welding parameters are listed in Table 2, the appearance and sizes of welded joint are shown in Fig.1.

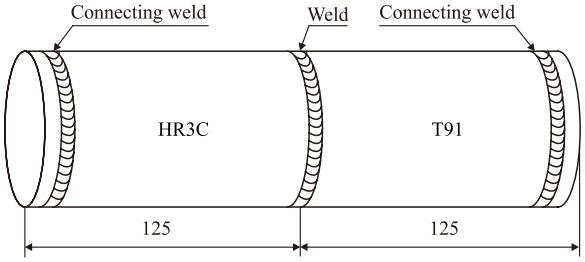

Fig.1 Appearance and size of the welded joint

2.2 Meshing scheme

The dimensions of FEM model were *Φ*57 mm × 7 mm × 250 mm, and weld widths on the outer surface and the inner surface were the same as those of welds in welding experiments, shown in Fig.1. Mesh size of the region near weld/T91 interface was the finest, the minimum size was 0.25 mm×1 mm, and the radian in radial direction was 10°, and the sizes of both sides on HAZ increased gradually, the size of the element away from HAZ was the largest, which was 2.2 mm×1 mm, and the radian in radial direction was also 10°. Nodes of the FEM model were 25 140, and elements were 21 312, meshing is shown in Fig.2(a). Data were taken along the longitudinal direction A_1A_2 and B_1B_2 of pipe on the outer surface and the inner surface and weld/T91 interface C_1C_2, as shown in Fig.2(b), respectively.

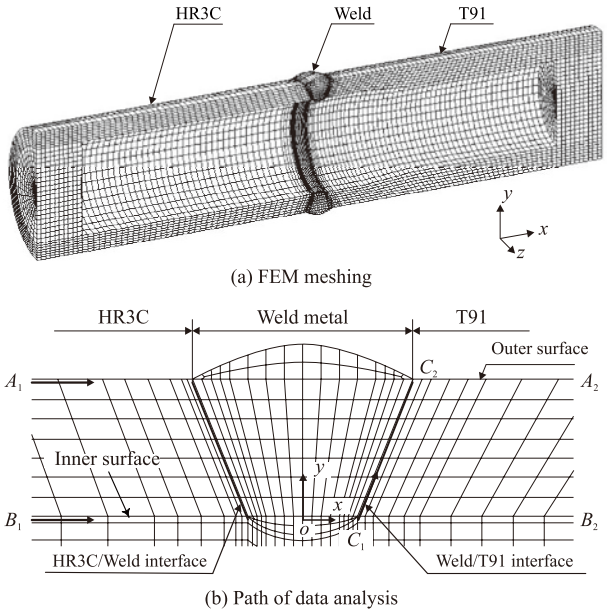

Fig.2 Meshing scheme and path of data analysis

2.3 Boundary conditions

A part of nodes at the left end of the model were fixed, and the displacements in the direction of *x, y, z* of fixed nodes were zero, in order to prevent creep specimen from moving or rotation, and the simulating results were not affected by the displacement constrain boundary conditions. The displacements in the direction of *y*, *z* of some nodes at the right end of the model were

Table 1 Chemical compositions of base metals and the filler metals/wt%

Item	C	Si	Mn	S	P	Cr	Mo	V	Nb	Ni	Al	N
HR3C	0.06	0.40	1.2			25.0			0.45	20.0		0.2
T91	0.10	0.40	0.46	0.010	0.010	8.85	0.93	0.21	0.09	0.01	0.003	0.038
ERNiCr-3	0.04	0.40	2.80	0.010	0.010	20.0	0.48	0.21	2.50	72.6		

Table 2 Welding parameters used in test

Welding layers	Welding passes	Welding current *I*/A	Welding voltage *U*/V	Welding speed v_w/(mm · min^{-1})	The volume of gas flow Q_1/(L · min^{-1})	The volume of gas flow in back side Q_2/(L · min^{-1})
1	1	91	8-10	20	10	10
2	2, 3	102	8-10	80	10	10
3	4, 5	102	8-10	80	10	
4	6, 7	102	8-10	80	10	
5	8, 9	102	8-10	70	10	

zero, in order to assure the convergence of simulation result and avoid deformation being too large. Applied load acted on the inner surface of the FEM model in the form of surface stress, and the stress level was 42.26 MPa. The simulation duration was 200 000 h, and the temperature was 873 K.

2.4 Constitutive equations of materials

Bailey-Norton creep law is used, and the equation is expressed as follows:

$$\dot{\varepsilon}^c = A\sigma^n \tag{1}$$

where A and n are creep coefficient and exponent of materials, and usually, A and n are constants.

Table 3 Material properties and creep parameters at 873 K

Materials	Yield strength R_{Cl}/MPa	Young's modulus E/GPa	Creep coefficient A	Creep exponent n
HR3C	480	190	2.6×10^{-29}	8.1
T91	458	185	2.51×10^{-28}	9.1
ERNiCr-3	478	190	7.9×10^{-30}	8.2

Mechanical properties and creep parameters at 873 K are listed in Table 3.

3 Results of numerical simulation

3.1 Maximum principal stress

The creep failure of dissimilar welded joints is the result of intergranular voids nucleation and propagation in the interfacial zone, and the creep voids are controlled by the maximum principal stress[10-12]. The maximum principal stress distributions along the outer surface (A_1A_2), the inner surface (B_1B_2) and interface (C_1C_2) are shown in Figs.3-5, respectively, when the internal pressure is 42.26 MPa. According to Fig.3, the maximum principal stress of HR3C/T91 joint on outer surface redistributes with the increase of simulation time. The maximum principal stresses in the vicinity of weld/T91 interface increase, and decrease in base metal HR3C. When t is 5 511 h, the maximum principal stress is 95.2 MPa in the vicinity of HR3C/weld interface (x=–6.31mm), 89.2 MPa at the HR3C/weld interface (x=–6 mm), 106.9 MPa in the vicinity of weld/T91 interface (x=5.5 mm), and 99.5 MPa at weld/T91 interface (x=6 mm), respectively. When t is 200 000 h, the maximum principal stresses in the vicinity of HR3C/weld interface and at HR3C/weld interface are 88.4 and 82.1 MPa, respectively. However, the maximum principal stresses in the vicinity of weld/T91 interface and at weld/T91 interface increase to 138.2 and 122.9 MPa, respectively. According to Fig.4, the maximum principal stresses in the vicinity of HR3C/weld and weld/T91 interface on inner surface increase with simulation time, and the maximum principal stresses in HR3C base metal decrease. When t is 5 511 h, the maximum principal stress is 156 MPa in the vicinity of HR3C/weld interface (x=–3.32 mm), and 155.5 MPa at the HR3C/weld interface(x=–3 mm). The maximum principal stress is 167.6 Mpa in the vicinity of weld/T91 interface (x=2.75 mm), and 148.2 Mpa at weld/T91 interface (x=3 mm). When t is 200 000 h, the maximum principal stresses in the vicinity of HR3C/weld interface and at HR3C/weld interface are 165.5 and 174.9 MPa, respectively. The

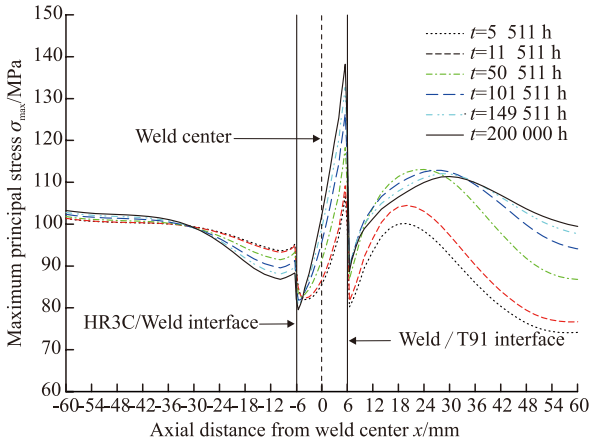

Fig.3 Distributions of maximum principal stresses along A_1A_2 on the outer surface

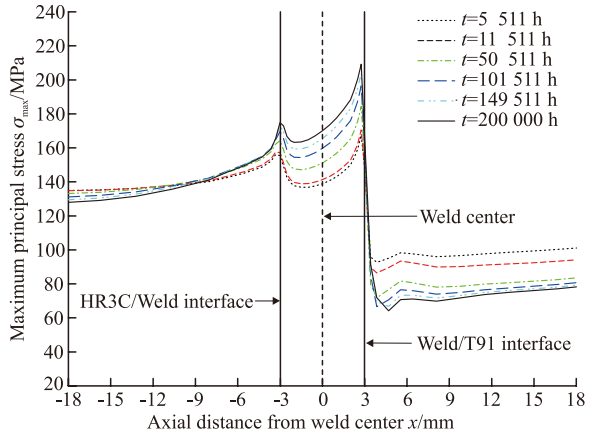

Fig.4 Distributions of maximum principal stresses along B_1B_2 in the inner surface

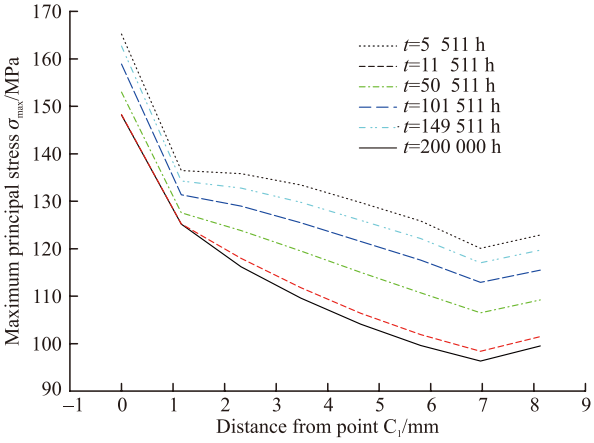

Fig.5 Distributions of maximum principal stresses along C_1C_2

maximum principal stresses in the vicinity of weld/T91 interface and at weld/T91 interface are 209.3 and 165.2 MPa, respectively. According to Fig.5, the maximum principal stresses in the weld/T91 interface increase with time, but, the increasing amplitude on the outer surface is different from that on the inner surface. The increasing amplitudes of the maximum principal stress on the outer surface and on the inner surface are 17 and 23.4 MPa, respectively. It follows that the maximum principal stress at the weld/T91 interface on the inner surface is quite high, and the material property degradation is extremely serious, the creep cavity is ease to come into being. Consequently, weld/T91 interface in the inner surface is the weakest location of the weld joint.

3.2 von Mises equivalent stress

Under the condition of applied stress of 42.26 MPa, distributions of von Mises equivalent stresses of the welded joint after simulation time ranging from 5 511 to 200 000 h, are shown in Fig.6-Fig.8, respectively. According to Fig.6, the peak of von Mises equivalent stress on the outer surface is in the vicinity of weld/T91 interface. When simulation time is 5 511 h, von Mises equivalent stresses are 96.5 MPa in the vicinity of weld/T91 interface(x=5.5 mm), 86.9 MPa at weld/T91 interface(x=6 mm) and 78.4 MPa at HR3C/ weld interface(x=−6 mm). And simulation time is 200 000 h, von Mises equivalent stresses are 139.9 Mpa in the vicinity of weld/T91 interface, 121.7 MPa at weld/T91 interface and 85.3MPa at HR3C/weld interface, respectively. According to Fig.7, the peak of von Mises equivalent stress on the inner surface is also in the vicinity of weld/T91 interface. When simulation time is 5 511 h, von Mises equivalent stress is 167.3 MPa in the vicinity of weld/T91 interface(x=2.75 mm), 154.4 MPa at weld/T91 interface (x=3 mm) and 165.6 MPa at HR3C/weld interface(x=−3 mm). And when simulation time is 200 000 h, von Mises equivalent stress is 204 Mpa in the vicinity of weld/T91 interface, 174.4 MPa at weld/T91 interface and 185.5 MPa at HR3C/weld interface, respectively. According to Fig.8, von Mises equivalent stresses at the weld/T91 interface increase with time, but, the increasing amplitude on the outer surface is different from that on the inner surface. The increasing amplitudes of the maximum principal stress on the outer surface and inner surface are 19.7 and 34.8 MPa, respectively. Thus it can be seen that von Mises equivalent stress in the vicinity of weld/T91 interface increases rapidly, and creep cavities are easy to expand. Therefore, weld/T91 interface is also the weakest region in HR3C/T91 joint.

3.3 Equivalent creep strain

Distributions of equivalent creep strains of joint after simulation operation from 5 511 to 200 000 h are shown in Fig.9-Fig.11. According to Fig.9, the creep deformation on the outer surface of HR3C/T91 welded joint concentrates in base metal T91, the main reason is that the resistance to deformation of HR3C and weld is higher than that of T91 steel. When simulation time is 5 511 h, the maximum equivalent creep strain(x=18 mm) is 0.002 53% and only 0.000 022 4% at the weld/ T91 interface (x=6 mm). When simulation time is 200 000 h, the maximum equivalent creep strain (x=22 mm) is 0.03% and only 0.003 82% at the weld/

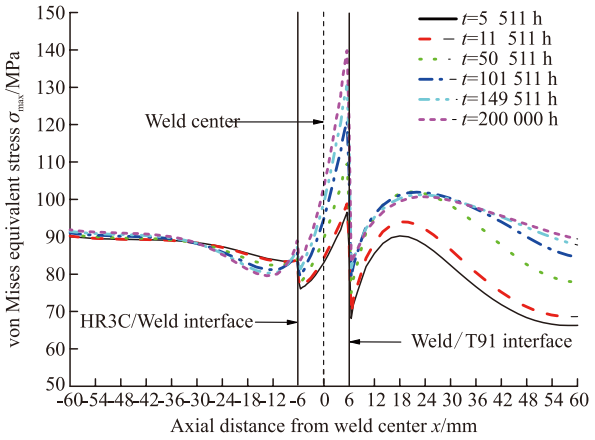

Fig.6 Distributions of von Mises equivalent stresses along A_1A_2 on the outer surface

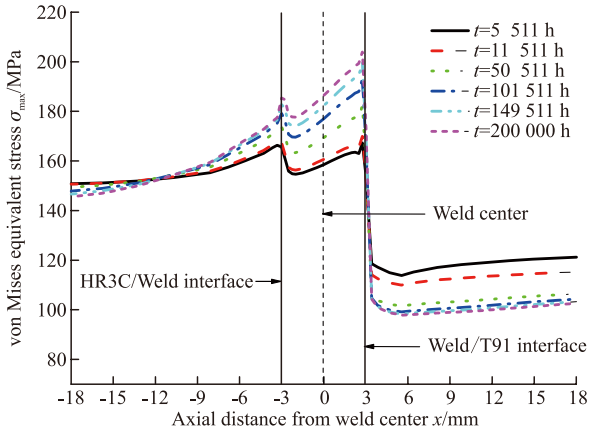

Fig.7 Distributions of von Mises equivalent stresses along B_1B_2 in the inner surface

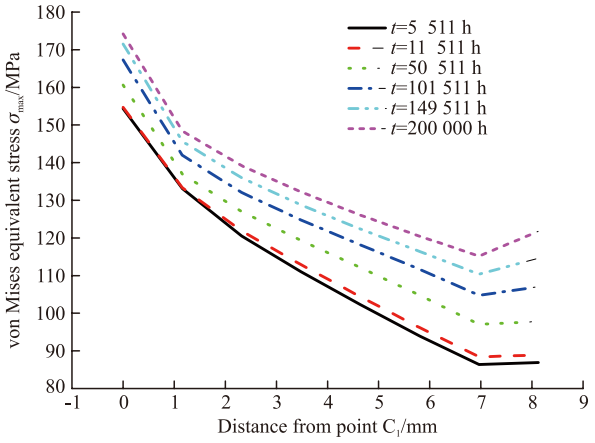

Fig.8 Distributions of von Mises equivalent stresses along C_1C_2

T91 interface (x=6 mm). According to Fig.10, the creep deformations on the inner surface of HR3C/T91 welded joint concentrate in base metal T91 and the vicinity of weld/T91 interface. When simulation time is 5 511 h, the maximum equivalent creep strains are 0.030 5% in T91 steel(x=24 mm) and 0.020 1% in the vicinity of weld/T91 interface(x=3.425 mm) and only 0.00736% at the weld/T91 interface(x=3 mm). When simulation time is 200 000 h, the maximum equivalent creep strains are 0.23% in T91 steel(x=26.02 mm) and 0.202% in the vicinity of weld/T91 interface and 0.084 4% at the weld/T91 interface. There is a creep constrain region close to weld/T91 interface, and the minimum equivalent creep strain(x=5.6 mm) is 0.129%. According to Fig.11, the equivalent creep strains of HR3C/T91 joint increase with time, but the increasing amplitude on the outer surface is different from that on the inner surface. The increasing amplitudes of the equivalent creep strains on the outer surface and on inner surface are 0.003 8% and 0.077 86%, respectively. Therefore, the distributions of the equivalent creep strain are quite complicated, and the equivalent creep strain can not accurately predict the creep life of HR3C/T91 joint.

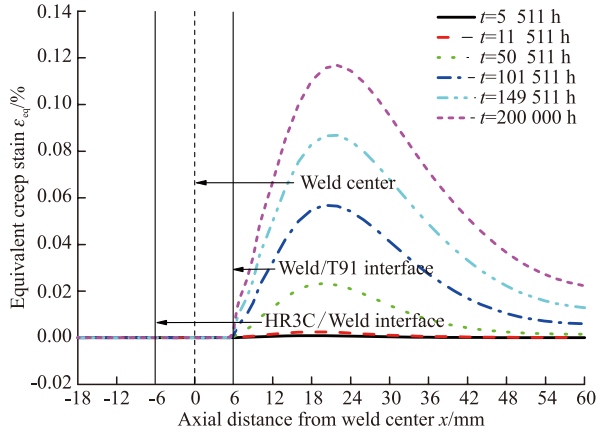

Fig.9 Distributions of equivalent creep strain along A_1A_2 on the outer surface

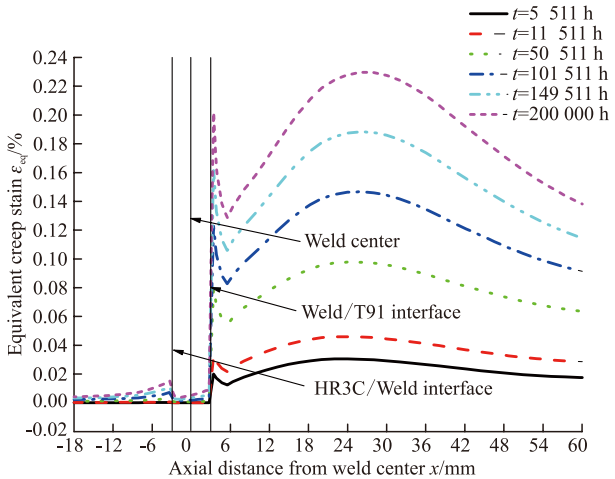

Fig.10 Distributions of equivalent creep strain along B_1B_2 in the inner surface

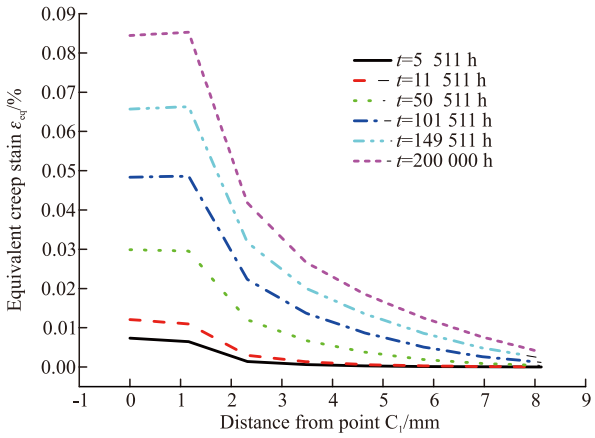

Fig.11 Distributions of equivalent creep strain along C_1C_2

3.4 Stress triaxiality

Stress triaxiality is expressed as follows:

$$R_\sigma = \frac{\sigma_m}{\sigma_{eq}} \tag{2}$$

where σ_m is the mean stress.

$$\sigma_m = \frac{1}{3}(\sigma_1 + \sigma_2 + \sigma_3) \tag{3}$$

$$\sigma_{eq} = \frac{\sqrt{2}}{2}\left[(\sigma_1-\sigma_2)^2 + (\sigma_2-\sigma_3)^2 + (\sigma_3-\sigma_1)^2\right]^{\frac{1}{2}} \tag{4}$$

σ_1, σ_2, and σ_3 are the first, second, and third principal stresses, respectively.

The distributions of stress triaxiality of joint after simulation time ranging from 5 511 to 200 000 h are shown in Fig.12-Fig.14. According to Fig.12, the peaks of stress triaxiality are located in the vicinity of HR3C/weld and weld/T91 interface on the outer surface and superposed with HR3C/weld and weld/T91 interface, and the peaks of stress triaxiality decrease with the increase of simulation time. When simulation time is 5 511 h, the stress triaxialities are 0.53 at HR3C/weld interface and 0.65 at weld/T91 interface. When simulation time is 200 000 h, the stress triaxialities are 0.31 at HR3C/weld interface and 0.36 at weld/T91 interface, respectively. According to Fig.13, the peaks of stress triaxiality are also located in the vicinity of HR3C/weld and weld/T91 interface on the inner surface and superposed with HR3C/weld and weld/T91 interface, and the stress triaxialities of weld and base metal T91 are comparatively low. When simulation time is 5 511 h, the stress triaxialities are 0.47 at HR3C/weld interface and 0.49 at weld/T91 interface. When simulation time is 200 000 h, the stress triaxialities are 0.53 at HR3C/weld interface and 0.52 at weld/T91 interface, respectively. According to Fig.14, the stress triaxiality R_σ of the weld/T91 interface on the inner surface increases with the increment of simulation time, and R_σ of weld/T91 interface on outer surface declines. The R_σ remains unchanged in the point of 4.9

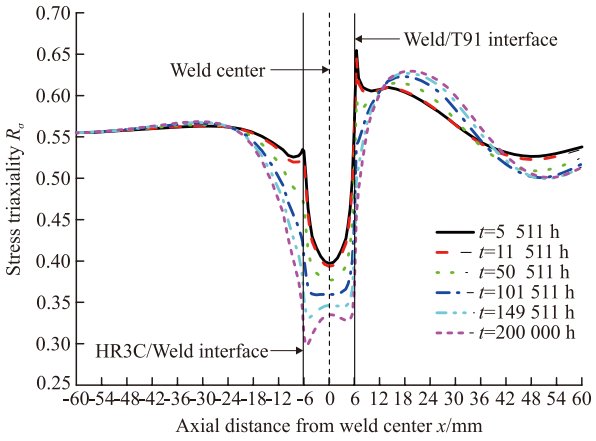

Fig.12 Distributions of stress triaxiality along A_1A_2 on the outer surface

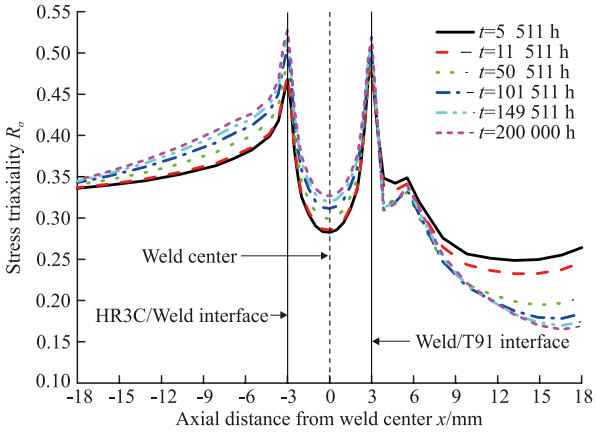

Fig.13 Distributions of stress triaxiality along B_1B_2 on the inner surface

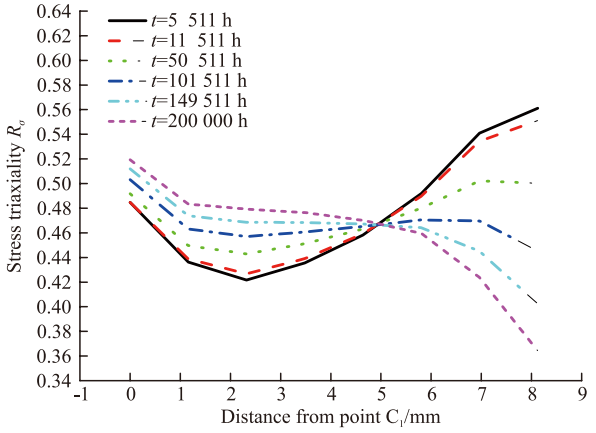

Fig.14 Distributions of stress triaxiality along C_1C_2

mm from C_1. Therefore, the weld/T91 interface within the range of 4.9 mm region from C_1 deteriorates in the simulation process, while the degradation process of weld/T91 interface outside the region of 4.9 mm from C_1 weakened. Thus, the weld/T91 interface on the inside surface is the weakest part in the joint since the creep strength of weld/T91 interface is greatly lower than that of HR3C/weld interface. It follows that the stress triaxiality can accurately describe the nucleation and expansion of creep cavities of HR3C/T91 joint.

4 Experimental

To verify the numerical simulation results, high temperature accelerated simulation test was designed to simulate the realistic service condition of DMWJ, the welded joint used for test is shown in Fig.1, two ends of specimens were sealed with HR3C and T91 steel, the distilled water was put into the tubes before tubes were sealed, then the specimens were put into a high temperature furnace, thus, distilled water becomes steam. The experimental temperature was 943 K, and simulating time was 5 012 h. The pressure of steam in tubes can be calculated by Formula (5).

$$(p+\frac{a}{V^2})(V-b)=RT \tag{5}$$

where a and b are constants; for steam, a=5.74 × 10^{-6} m^6·atm/mol^2; b=30.5 × 10^{-6} m^3/mol; P is the internal pressure of steam in tube; V is the volume of tube; R is the universal gas constant; and T is the experimental temperature in Kelvin.

The inner pressure in the pipe welded joint is 42.26 MPa by thermodynamic calculation, and the correlation between the test temperature and time can be calculated by Larson-Miller formula:

$$P(\sigma)=T(C+\log t) \tag{6}$$

where $P(\sigma)$ is the equivalency parameter; t is the time at temperature T; it was found that the value of constant C was 25 for T91 steel.

The microstructure of CGHAZ(coarse grained heat affected zone) close to weld/T91interface in base metal T91 is tempered martensite, the lath feature of martensite is remained entirely after welding, as shown in Fig.15. After accelerated simulating operation for 5 012 h, the lath feature of martensite in CGHAZ disappears obviously, and grain boundaries coarsen, as shown in Fig.16. Cracks are found along the weld/T91 interface of the inner surface, and the appearance of interfacial crack is shown in Fig.17. Owing to the creep strength mismatching between weld metal and base material T91, this will lead to strenuous constraint in the side of steel T91 adjacent to weld. Cracking initiates in T91/weld interface of the inner surface, and develops along the radial and loop direction of the joint. Finally, failure of HR3C/T91 joint occurs. The fracture appearance of T91/weld interface after accelerated operation for 5 012 h is shown in Fig.18. According to Fig.18, it is seen that cracking comes into being mainly by the connection of creep voids. The fracture mode is grain boundary rupture. The weld/T91 interface is seriously damaged after accelerated operation for 5 012

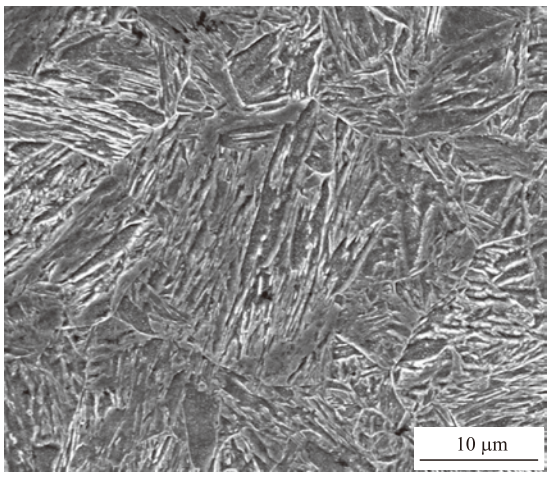

Fig.15 Microstructures of CGHAZ near weld/T91 interface before accelerated operation

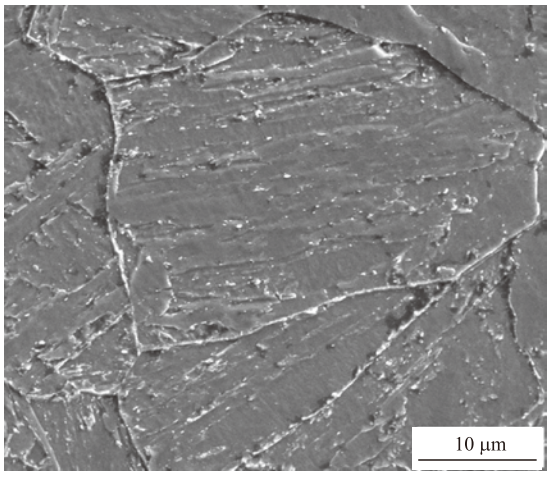

Fig.16 Microstructures of CGHAZ near weld/T91 interface before accelerated operation

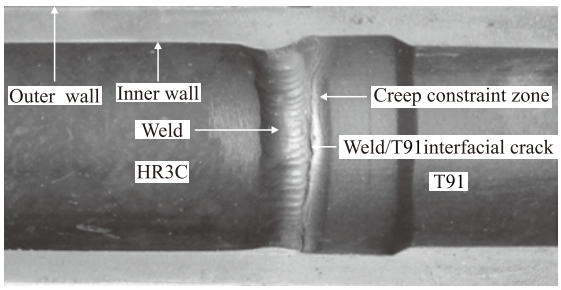

Fig.17 Appearance of the interfacial crack after accelerated operation for 5 012 h

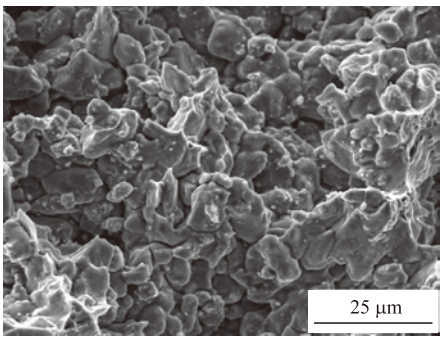

Fig.18 Fracture appearance of weld/T91 interface after accelerated operation for 5 012 h

h, premature interfacial creep failure occurred at weld/T91 welding interface. The experimental results are in good agreement with those of numerical simulation. Therefore, weld/T91 interface is the weakest region of the welded joint.

5 Conclusions

a) The peak of maximum principal stress is in the vicinity of weld/T91 interface, and creep cavities are easy to form.

b) The peak of von Mises equivalent stress is in the vicinity weld/T91 interface, and creep cavities are easy to expand.

c) The peaks of stress triaxialities are located in the vicinity of HR3C/weld and weld/T91 interface and superposed with HR3C/weld and weld/T91 interface, and the stress triaxiality of weld/T91 interface is comparatively high, accordingly, weld/T91 interface is the weakest position of HR3C/T91 joint. Stress triaxiality can accurately describe the nucleation and expansion of creep cavities of HR3C/T91 joint.

d) There are two peaks of equivalent creep strain, and creep deformation distribution is quite complicated, the maximum equivalent creep strain is in the place 27-32 mm away from the weld/T91 interface, and there exists a creep constrain region in the vicinity of weld/T91 interface.

References

[1] Yang F, Zhang Y L, Ren Y N, *et al*. *New Heat-resistant Steel Welding*[M]. Beijing: China Electric Power Press, 2006 (in Chinese)

[2] Ning B Q, Liu Y C, Yin H Q, *et al*. Development and Investigation of Ferritic Heat Resistant Steels for Boiler Tube of the Advanced Power Plants[J]. *Mater. Rev.*, 2006,20(12):83-86 (in Chinese)

[3] Swindemana R W, Santellaa M L, Maziasza P J, *et al*. Issues in Replacing Cr-Mo Steels and Stainless Steels with 9Cr–1Mo–V Steel[J]. *Int. J. Pressure Vessels and Piping*, 2004, 81(6):507-512

[4] Zhu L H, Zhao Q X, Gu H C, *et al*. Evaluation of Creep Rupture Lifetime of New Heat-resistant Steel T91[J]. *Boiler Technology*, 2002,33(5):24-27 (in Chinese)

[5] Brozda J, Lomozik M , Zeman M. Weldability of 9Cr1MoNbV(P91) Steel Intended for Service in the Power Industries[J]. *Welding Research Abroad*, 1997,43(8-9):58-68

[6] Roberts D I, Ryder R I, Viswanathan R. Performance of Dissimilar Welds in Service[J]. *Journal of Pressure Vessel Technology*, 1985,107(3):247-254

[7] Lundin C D. Dissimilar Metal Welds-transition Joints Literature Review[J]. *Welding Journal*, 1982, 61(Suppl.2): 58-63

[8] Bhaduri A K, Venkadesan S, Rodriguez P. Transition Metal Joints for Steam Generators-an Overview[J]. *Int. J. Pres. Ves. & Piping*, 1994, 58(3): 251-265

[9] Zhang J Q, Zhang G D, He J, *et al*. Behaviors of Interfacial Creep Damage of Dissimilar Welded Joint between Martensitic Heat-resistant Steel and Bainitic Heat-resistant Steel[J]. *Acta Metall. Sin*., 2007, 43(23): 1 275-1 281

[10] Zhang J Q, Zhang G D, Luo C H, *et al*. Influence of Creep Strength of Weld on Interfacial Creep Damage of Dissimilar Welded Joint between Martensitic and Bainitic Heat-resistant Steel[J]. *Journal of Wuhan University of Technology-Mater. Sci. Ed.*, 2013, 28(1): 178-183

[11] Shi C Y, Tian X T, Chen Z G. On Mechanical Parameter Controlling Creep Brittle Rupture Along Interface of Dissimilar Metal Welded Joints[J]. *Transactions of the China Welding Institution*, 1995, 16(4):185-189 (in Chinese)

[12] Cane B J, Middleton C J. Intergranular Creep-cavity Formation in Low-alloy Bainitic Steels[J]. *Metal Science,* 1981, 15: 295-301